Cross-talk between the methylerythritol phosphate and mevalonic acid pathways of isoprenoid biosynthesis in poplar

Hui Wei[1, †], Ali Movahedi[1, †], Chen Xu[1,2, †], Weibo Sun[1], Pu Wang[1], Dawei Li[1], and Qiang Zhuge[1, *]

[1] Co-Innovation Center for Sustainable Forestry in Southern China, Key Laboratory of Forest Genetics & Biotechnology, Ministry of Education, College of Biology and the Environment, Nanjing Forestry University, Nanjing 210037, China

[2] Jiangsu Provincial Key Construction Laboratory of Special Biomass Resource Utilization, Nanjing Xiaozhuang University, Nanjing 211171, China

* Correspondence: qzhuge@njfu.edu.cn; Fax: +86-25-8542-8701

† These authors are contributed equally to the first author.

Abstract

Plants use two distinct isoprenoid biosynthesis pathways: the methylerythritol phosphate (MEP) pathway and mevalonic acid (MVA) pathway. 1-deoxy-D-xylulose5-phosphate synthase (DXS) and 1-deoxy-D-xylulose5-phosphate reductoisomerase (DXR) are the rate-limiting enzymes in the MEP pathway, and 3-hydroxy-3-methylglutaryl-CoA reductase (HMGR) is a key regulatory enzyme in the MVA pathway. Previously, overexpression of *Populus trichocarpa PtDXR* in Nanlin 895 poplar was found to upregulate resistance to salt and drought stresses, and the transgenic poplars showed improved growth. In the present study, *PtHMGR* overexpressors (OEs) exhibited higher expression levels of *DXS*, *DXR*, 1-hydroxy-2-methyl-2-(E)-butenyl-4-diphosphate synthase (*HDS*), and 1-hydroxy-2-methyl-2-(E)-butenyl-4-diphosphate reductase (*HDR*) and lower expression levels of 2-C-methyl-d-erythritol4-phosphate cytidylyltransferase (*MCT*), 4-diphosphocytidyl-2-C-methyl-D-erythritol kinase (*CMK*), and 3-hydroxy-3-methylglutaryl-coenzyme A synthase (*HMGS*) than non-transgenic poplars (NT). However, the poplar *PtDXR*-OEs showed upregulated expression levels of MEP-related genes and downregulated expression of MVA-related genes. Moreover, overexpression of *PtDXR* and *PtHMGR* in poplars caused changes in MVA-derived trans-zeatin-riboside (TZR), isopentenyl adenosine (IPA), castasterone (CS) and 6-deoxocastasterone (DCS), as well as MEP-derived carotenoids, gibberellins (GAs), and abscisic acid (ABA). In *PtHMGR-OE*s, greater accumulation of geranyl diphosphate synthase (*GPS*) and geranyl pyrophosphate synthase (*GPPS)* transcript levels in the MEP pathway led to accumulation of MEP-derived isoprenoids, while upregulation of farnesyl diphosphate synthase (*FPS*) expression in the MVA pathway contributed to increased levels of MVA-derived isoprenoids. Similarly, in *PtDXR*-OEs, increased *GPS* and *GPPS* transcript levels in the MEP pathway boosted MEP-derived isoprenoid levels and changes in *FPS* expression affected MVA-derived isoprenoid yields. From these results, we can conclude that cross-talk exists between the MVA and MEP pathways.

Keywords: MEP; MVA; poplar; terpenoids; cross-talk

1. Introduction

In plants, terpenoids including abscisic acid (ABA), gibberellins (GAs), carotene, lycopene, cytokinins (CKs), strigolactones (GRs), and brassinosteroids (BRs) are produced via the methylerythritol phosphate (MEP) and mevalonic acid (MVA) pathways (van *et al*., 2006; Xie *et al*., 2008; Henry *et al*., 2015). These MEP- and MVA-derived terpenoids are involved in plant growth and development, as well as in the response to environmental changes (Kirby & Keasling, 2009; Bouvier *et al*., 2009). The conversion of isopentenyl diphosphate (IPP) into dimethylallyl diphosphate (DMAPP) catalyzed by isopentenyl diphosphate isomerase (IDI) provides the fundamental materials for production of all isoprenoids (Hemmerlin *et al*., 2012; Lu *et al*., 2012; Zhang *et al*., 2019). In addition, IPP and DMAPP play roles in communication (cross-talk) between the MEP and MVA pathways, and previous research has shown that cross-talk occurs between the MEP and MVA pathways (Huchelmann *et al*., 2014; Liao *et al*., 2016).

The MVA pathway occurs in the cytoplasm, ER, as well as peroxisomes and produces sesquiterpenoids and sterols. 3-hydroxy-3-methylglutaryl-CoA reductase (HMGR), which is a rate-limiting enzyme in the MVA pathway can catalyze 3-hydroxy-3-methylglutary-CoA (HMG-CoA) to form MVA (Cowan *et al*., 1997; Roberts *et al*., 2007). In addition, the MEP pathway occurs in the chloroplast and is responsible for producing carotenoids, ABA, GAs, and diterpenoids. 1-deoxy-D-xylulose5-phosphate synthase (DXS) and 1-deoxy-D-xylulose5-phosphate reductoisomerase (DXR) are rate-limiting enzymes in the MEP pathway that catalyze D-glyceraldehyde3-phosphate (D-3-P) and pyruvate to form 2-C-methyl-D-erythritol4-phosphate (MEP) (Wang *et al*., 2012; Yamaguchi *et al*., 2018). Terpenoids in plant cells are involved in diverse cellular processes. Sesquiterpene derivatives such as phytoalexin and volatile oils play important roles in plant growth, development, and disease resistance (Hain *et al*., 1993; Ren *et al*., 2008). α-Tocopherol (vitamin E) is an antioxidant that improves human health (Weber *et al*., 1997). Sterols are an important component of biological membranes, which are linked to metabolism (Huang *et al*., 2008). Photosynthetic pigments participate in plant photosynthesis and enable the conversion of basic carbon sources for plant growth (Esteban *et al*., 2015). Plant hormones (such as ABA and GAs) are connected to plant growth and the responses to biotic and abiotic stresses (Kazan *et al*., 2015). Paclitaxel is one of the most effective chemotherapy agents for cancer treatment, and artemisinin is an anti-malarial drug (Kong *et al*., 2015; Kim *et al*., 2016).

Previous metabolic engineering studies have proposed strategies for improving the yields of specific metabolites in plants. For example, industrial exploitation of hairy roots has been used to enhance secondary metabolite production (Zhang *et al*., 2004; Rahman *et al*., 2009). 3-Hydroxy-3-methylglutaryl-coenzyme A synthase (HMGS) is a second enzyme that has been genetically engineered to improve terpenoid content. For example, overexpression of *Brassica juncea HMGS* in tomato plants leads to upregulated carotenoid and phytosterol levels (Liao *et al*., 2018). HMGR can be metabolically engineered to regulate the content of terpenoids (Aharoni *et al*., 2005; Dueber *et al*., 2009). In *Arabidopsis thaliana*, HMGR1 has been shown to play an important role in the biosynthesis of sterols and triterpenoids through investigation of *A. thaliana* mutant lines (Suzuki *et al*., 2005). Moreover, overexpression of *PgHMGR1* from ginseng in *A. thaliana* can lead to increased production of sterols and triterpenes (Kim *et al*., 2014). Transgenic tobacco overexpressing the *HMGR* of *Hevea brasiliensis* has elevated levels of phytosterol (Schaller *et al*., 1995). Dai *et al*. (2011) expressed *SmHMGR2* in *Salvia miltiorrhiza*, resulting in improvement of squalene and tanshinone contents. Interestingly, transgenic T_0 tomato fruits display elevated levels of phytosterol with overexpression of *HMGR1* from *A. thaliana*, but only certain phytosterols increase in mature T_2 fruits (Enfissi *et al*., 2005). DXR can be genetically engineered to regulate the content of terpenoids and expressed *DXR* in *Arabidopsis* and observed enhanced flux through the MEP pathway (Carretero-Paulet *et al*., 2006). Overexpression of *A. thaliana DXR* in *Salvia sclarea* hairy roots increases levels of anthiolimine, a diterpene (Vaccaro *et al*., 2014). Overexpression of *DXR* in peppermint affects regulation of monoterpenes in leaf tissues (Mahmoud *et al*., 2001). Farnesyl diphosphate is the synthetic precursor of numerous primary metabolites including steroids, polyterpenoid alcohols, and ubiquinone, and represents the branching point of many terpenoid metabolic pathways (Wong *et al*., 2018). In summary, overexpression of genes in the MEP and MVA pathways by means of metabolic engineering can change the expression levels or activities of related enzymes and metabolic products, which opens up a new direction for plant breeding and acquisition of metabolic products.

To date, most studies have found that the MVA and MEP pathways are located in different parts of plants. The MVA pathway occurs in the cytoplasm and endoplasmic reticulum and involves the biosynthesis of secondary metabolites such as sterols, sesquiterpenes, and triterpenes. Meanwhile, the MEP pathway takes place in plastids and mainly involves the biosynthesis of diterpenes, monoterpenes, carotenoids, and isoprene. Previous studies have

shown that the MVA and MEP pathways do not operate in isolation, and that some metabolic intermediates that link them can be exchanged through plastid membranes (Laule *et al*., 2003; Liao *et al*., 2006). In this study, to comprehensively investigate such cross-talk in poplar, we determined the transcript levels of MEP- and MVA-related genes in *PtHMGR*-OEs and *PtDXR*-OEs. The results showed that not only were the transcript levels of MVA-related genes (such as acetoacetyl CoA thiolase [*AACT*], mevalonate kinase [*MVK*], and mevalonate 5-diphosphate decarboxylase [*MVD*]) upregulated in *PtHMGR*-OEs, but also the expression levels of MEP-related genes (such as *DXS*, *DXR*, *HDS*, and *HDR*) were improved. In *PtDXR*-OEs, the transcript levels of MVA-related genes were downregulated, while the expression levels of MEP-related genes were increased. Based on these results, we propose that the MEP pathway is dominant and the MVA pathway is subordinate. Overexpression of *PtDXR* in poplar increases the expression levels of MEP-related genes, which may result in the accumulation of terpenoids, and then feedback with the MVA pathway may lead to inhibited expression of MVA-related genes. In addition, the transcript levels of MEP-related genes and products, such as MEP-derived isoprenoids, were affected in *PtHMGR*-OEs. These results demonstrate that cross-talk occurs between the MEP and MVA pathways.

2. Results

2.1. Isolation of the *PtHMGR* gene and characterization of transgenic poplars

The *PtHMGR* gene (Potri.004G208500.1) was isolated from *P. trichocarpa*. The amino acid sequence of PtHMGR contains similar domains, including HMG-CoA-binding motifs (EMPVGYVQIP' and 'TTEGCLVA) and NADPH-binding motifs (DAMGMNMV' and 'VGTVGGGT) (Ma *et al.*, 2012) (Supplemental Figure 1).

In addition, the results of Southern blotting indicated a copy number of at least three copies for *PtHMGR* in the poplar genome (Figure 1A). As shown in Figure 1B, probe 2 could specifically recognize *PtHMGR* (Potri.004G208500.1), indicating that the probe 2 used for qRT-PCR of *PtHMGR* could be applied to the follow-up study of *PtHMGR* expression levels. Based on the whole genome of 10 species achieved from Phytozome, an evolution tree was constructed and showed the evolution relationship of those species (Figure 2A). Also, the phylogenetic tree illustrated that the function and evolution of the HMGR family is relatively strongly conserved among all plants (Figure 2B). In addition, the HMGR originated from a single ancestor and evolved into two different groups, one each in monocotyledons and dicotyledons (Ferrero *et al*., 2015; Li *et al*., 2014). This result shows that evolutionary tree

constructed from HMGR is consistent with that constructed from the whole genomes of various species (Figure 2).

Analyses of gel electrophoresis illustrated that the *PtHMGR* gene was inserted into the genome of "Nanlin 895" plants obtained through screening with kanamycin (Kan) using the primer for the cauliflower mosaic virus (CaMV) 35S promoter (Supplemental Table 1) as the forward primer and that for *PtHMGR*-R (Supplemental Table 1) as the reverse primer (Supplemental Figure 1). In addition, the transcript levels of *PtHMGR* were higher in transgenic lines than in NT plants, showing that *PtHMGR* could be stably expressed in Nanlin 895 plants (Supplemental Figure 2). Overall, *PtHMGR* was inserted into poplar chromosomes and expressed in poplar cells.

2.2. Effects of *PtHMGR* overexpression on the expression levels of MVA- and MEP-related genes in poplar *PtHMGR*-OE seedlings

MVA-related genes (*AACT*, *HMGS*, *MVK*, and *MVD*) were significantly upregulated in *PtHMGR*-OE3 and *PtHMGR*-OE7 relative to NT poplars (Figure 3). The expressions of MEP-related genes (*DXS*, *DXR*, *HDS*, *HDR*, *MCT*, and *CMK*) were also increased in *PtHMGR*-OE3 and *PtHMGR*-OE7 relative to NT poplars (Figure 3). Moreover, the expression levels of genes (*FPS*, *IDI*, *GPS*, and *GPPS*) involved in the biosynthesis of C10 and C20 universal isoprenoid precursors were significantly elevated in *PtHMGR*-OE3 and *PtHMGR*-OE7 (Figure 3).

2.3. *PtDXR* overexpression affects expression levels of MVA- and MEP-related genes in transgenic poplars

When determining the transcript levels of MVA- and MEP-related genes in *PtDXR*-OE1–1 and *PtDXR*-OE3–1 via qRT-PCR, we found that the expression levels of *DXS*, *HDS*, *HDR*, *MCT*, and *CMK* genes involved in the MEP pathway were significantly greater in transgenic poplars. Notably, MVA-related genes (*AACT*, *HMGS*, *HMGR*, *MVK*, *MVD*) were downregulated in *PtDXR*-OE seedlings (Figure 4), the opposite of the MVA-related gene expression results obtained from *PtHMGR*-OEs. In addition, the expression levels of *FPS*, *IDI*, *GPS*, and *GPPS* were significantly elevated in both *PtDXR*-OE1–1 and *PtDXR*-OE3–1 compared to the NT poplars (Figure 4).

2.4. Overexpression of *PtHMGR* leads to accumulation of MVA-derived TZR, IPA, and DCS as well as MEP-derived carotenoids, ABA, and GAs

Analyses of carotenoids, ABA, GAs, zeatin, TZR, IPA, CS, and DCS, which are involved

in plant growth and development as well as the responses to biotic and abiotic stresses, would help to elucidate plant growth and the stress response process and could guide poplar breeding. The HPLC-MS/MS chromatograms of ABA, GA, zeatin, TZR, IP, IPA, CS, and DCS standards are provided in Supplemental Figures 3–13.

The expression levels of ABA synthesis-related genes including 9-cis-epoxycarotenoid dioxygenase (*NCED*) and zeaxanthin epoxidase (*ZEP*) in *HMGR*-OE and NT leaves were analyzed via qRT-PCR, and ABA contents of *PtHMGR*-OE and NT leaves were analyzed via HPLC-MS/MS. The transcript levels of *NCED1*, *NCED3*, *NCED5*, *NCED6*, *ZEP1*, *ZEP2*, and *ZEP3* in *PtHMGR*-OE poplars were elevated compared to that in NT poplars (Figure 3). In addition, ABA levels were significantly elevated in lipid extracts from *HMGR*-OE poplar leaves (Figure 5). The contents of β-carotene and lycopene, which are intermediate products in the synthesis of ABA, were identified via HPLC, and the results showed significant enhancement of each in *HMGR*-OE leaves (Figure 5) Lutein content was also significantly elevated in *HMGR*-OE leaves (Figure 5). In addition, the total level of GA3, a downstream product of MEP, increased to 0.2–0.35 ng/g in *PtHMGR*-OE leaves, compared to 0.08–0.1 ng/g in NT leaves (Figure 6A). Among MVA-related factors, the results of HPLC-MS/MS showed that the TZR and IPA contents were higher in *PtHMGR*-OEs than in the NT (Figure 6B, and C). The DCS content of *PtHMGR*-OEs increased to 0.31–0.41 ng/g relative to 0.74–1.12 ng/g in the NT (Figure 6D), representing an average 3-fold increase in *PtHMGR*-OEs. However, the CS content showed the opposite result in the comparison between *PtHMGR*-OEs and NT (Figure 6E). Together, these results illustrate that the *HMGR* gene not only causes changes in MVA-related genes and their products, but also affects MEP-related genes and products. Meanwhile, zeatin, IP, GA1, GA4, and GA7 were not detected through HPLC-MS/MS (Supplemental Figure 14).

2.5. Enhanced TZR, IPA, DCS, carotenoid, ABA, and GA3 levels in *PtDXR*-OE poplars

The levels of β-carotene, lycopene, and ABA were much higher in *PtDXR*-OE poplars than in NT plants, and lutein, which is considered a MEP-derived hormone, showed a similar result (Figure 7). When the molecular mechanism underlying the improvement of ABA in *PtDXR*-OEs was investigated, the expression levels of *NCED1*, *NCED3*, *NCED5*, *NCED6*, *ZEP1*, *ZEP2*, and *ZEP3* were significantly higher in *PtDXR*-OEs than in NT plants (Figure 7). In addition, a significant increase in GA3 in *PtDXR*-OEs was observed through HPLC-MS/MS analyses (Figure 8A). In addition to upregulating MEP-derived products, overexpression of

PtDXR also affected the contents of MVA-derived products. The TZR content of *PtDXR*-OEs increased to 0.24–0.37 ng/g compared to 0.0274–0.033 ng/g in NT plants (Figure 8B), representing an average 10-fold increase in *PtDXR*-OEs. The content of IPA in *PtDXR*-OEs increased to 0.84–1.12 ng/g, compared to 0.32–0.41 ng/g in NT poplars (Figure 8C), representing an average 3-fold increase in *PtDXR*-OEs. The DCS content of *PtDXR*-OEs was also significantly higher. Its level increased to 3.06–3.62 ng/g, with only 1.47–1.52 ng/g in NT plants (Figure 8D), representing an average 3-fold increase in *PtDXR*-OEs (Figure 8D). By contrast, the content of CS in *PtDXR*-OEs significantly decreased compared to that in NT poplars (Figure 8C), indicating significant downregulation in *PtDXR*-OEs (Figure 8E). We were unable to determine the contents of zeatin, IP, GA1, GA4, and GA7 through HPLC-MS/MS (Supplemental Figure 15).

3. Discussion

3.1. Characterization and evolutionary history of HMGR

Previous studies have shown that *NtHMGR2* is a stress-responsive gene, whereas *NtHMGR1* is a housekeeping gene (Hemmerlin *et al*., 2004; Merret *et al*., 2007). *LcHMGR1* is most highly expressed during the early stages of fruit development and is involved in the regulation of fruit size. The level of *LcHMGR1* expression is higher and lasts longer in larger fruits, while *LcHMGR2* is expressed most highly during the late stages of fruit development and is related to the biosynthesis of isoprenoid substances required for cell elongation during that time (Rui *et al*., 2012). The expression of *CaHMGR1* is temporary and tissue-specific, whereas that of *CaHMGR2* is constitutive. *CaHMGR1* is only expressed in fruit tissues (pulp, endosperm, and endocarp), flower buds, and leaves during the initial stages of development, while *CaHMGR2* is expressed in all tissues (flower buds, leaves, branches, and roots) and fruit tissues at various stages of development (Tiski *et al*., 2012). In this study, we found that there is a copy number of at least three for *PtHMGR* genes in the poplar genome, and that the *PtHMGR* gene (Potri.004G208500.1) has high homology with other known *HMGR1* genes based on multiple alignment analyses. In addition, the whole genome and HMGR protein sequences of various species were used to construct evolutionary trees, and the resulting evolutionary relationships among species were similar. Because *HMGR* in plants is a relatively conserved gene in the MVA pathway, it should be considered an important factor in studies of biological genetic differentiation and molecular evolution, and can be used as a reference for determining relationships among species.

3.2. HMGR regulates isoprenoid biosynthesis genes in *PtHMGR*-OE plants

Liao *et al*. (2018) showed that overexpression of *BjHMGS1* affects the expression levels of MEP- and MVA-related genes and slightly increases the transcript levels of *DXS* and *DXR* in transgenic plants. However, the expression levels of *DXS*, *DXR*, *HDS*, and *HDR* are significantly improved in *PtHMGR*-OE poplars, while those of *MCT* and *CMK* are downregulated. In addition, overexpression of *BjHMGS1* in tomato causes the expression levels of *GPS* and *GPPS* to significantly increase (Liao *et al*., 2018). In the present study, we also investigated the expression levels of *FPS*, *GPS*, and *GPPS*, and overexpression of *PtHMGR* increased their expression levels, which may have enhanced the interaction between IPP and dimethylallyl diphosphate (DMAPP), thereby increasing the biosynthesis of plastidial C15 and C20 isoprenoid precursors.

Xu *et al*[46] showed that overexpression of the *HMGR* gene in *Ganoderma lucidum* causes no significant changes in farnesyl diphosphate synthase (*FPS*), squalene synthase (*SQS*), or lanosterol synthase (LS) mRNA expression, despite increasing the contents of squalene and lanosterol. Overexpression of *BjHMGS1* in tomato significantly increases transcript levels of *FPS*, *SQS*, squalene epoxidase (*SQE*), and cycloartenol synthase (*CAS*) (Liao *et al*., 2018). Notably, the transcript levels of *AACT*, *MVK*, and *MVD* are significantly upregulated in *PtHMGR*-OE poplars although the expression level of *HMGS* is reduced. Increased expression has been observed for most MVA-related genes that contribute to the biosynthesis of sesquiterpenes and other C15 and universal C20 isoprenoid precursors.

3.3. Overexpression of *PtDXR* affects MEP- and MVA-related genes in *PtDXR*-OE plants

Overexpression of *TwDXR* in *Tripterygium wilfordii* increases the expression levels of *TwHMGS*, *TwHMGR*, *TwFPS*, and *TwGPPS*, but decreases that of *TwDXS* (Zhang *et al*., 2018). Overexpression of *NtDXR1* in tobacco increases the transcript levels of eight MEP-related genes, indicating that overexpression of *NtDXR1* could lead to upregulated expression of downstream genes in the MEP pathway (Zhang *et al*., 2015). Changes in the *DXR* transcript level of transgenic *A. thaliana* do not affect *DXS* gene expression or enzyme accumulation, although overexpression of *DXR* boosts MEP-derived isoprenoids such as carotenoids, chlorophylls, and taxadiene in *A. thaliana* (Carretero-Paulet *et al*., 2015). Overexpression of the potato *DXS* gene in *A. thaliana* can cause upregulation of the downstream *GGPPS* gene and *PSY* (phytoene synthase) gene (Henriquez *et al*., 2016). In addition, transformation of the *DXS* gene from *A. thaliana* into *Daucus carota* significantly enhances the expression level of the

PSY gene (Simpson *et al*., 2016).

Our results show both similarities and differences compared to previous studies. For example, we found that the transcript levels of MEP-related genes were higher in *PtDXR*-OE poplars than in NT poplars. However, overexpression of *PtDXR* in poplar led to significantly downregulated expression levels of MVA-related genes. Together, these findings illustrate that carbon sources may be preferentially synthesized into monoterpenes, diterpenes, and tetraterpenoids in poplar cells. Secondary metabolic pathways in plants are tightly regulated by the transcript levels of MEP- and MVA-related genes. The dominant isoprenoid compounds synthesized in different plants differ greatly. The regulation of the expression of multiple enzymes largely controls whether specific secondary metabolites are synthesized and to what extent. The diversity of biosynthetic pathways, the complexity of metabolic networks, and the unknown regulation of gene expression lead to very different regulation pattenrs of MEP- and MVA-related gene expression among species. One possible conclusion is that MEP- and MVA-related genes often do not work alone, but instead are co-expressed with upstream and downstream genes in the MEP and MVA pathways to carry out a specific function.

3.4. Overexpression of *HMGR* promotes formation of ABA, GAs, and carotenoids in plastids and accumulation of TZR, IPA, DCS in the cytoplasm

Plant HMGR, as the rate-limiting enzyme in the MVA pathway, plays a very important role in controlling the flow of carbon in that metabolic pathway. Upregulation of the *HMGR* gene significantly increases isoprenoid levels in plants. Studies on homologous and heterologous overexpression of *HMGR* have reported significantly elevated levels of isoprenoid in transgenic plants. In one study, *Hevea brasiliensis HMGR1* was transferred into tobacco, and it increased the sterol content of transgenic tobacco as well as the accumulation of intermediate metabolites (Schaller *et al*., 1995). In another study, *A. thaliana HMGR* overexpression in *Lavandula latifolia* increased the levels of sterols in the MVA pathway and of MEP-derived monoterpenes and sesquiterpenes (Munoz-Bertomeu *et al*., 2007). In still another, overexpression of the *SmHMGR* gene in hairy roots increased MEP-derived diterpene tanshinone (Kai *et al*., 2011). In our study, ABA synthesis-related genes (*NCED1*, *NCED3*, *NCED5*, *NCED6*, *ZEP1*, *ZEP2*, and *ZEP3*) and the contents of ABA, GA3, and carotenoids were upregulated in *PtHMGR*-OE poplar seedlings, suggesting that overexpression of *HMGR* may indirectly affect the biosynthesis of MEP-related isoprenoids including ABA, GAs, and carotenoids. The accumulation of MVA-derived isoprenoids including TZR, IPA, and DCS

was significantly elevated in *PtHMGR*-OEs, indicating that *PtHMGR* overexpression has a direct influence on the biosynthesis of MVA-related isoprenoids. Therefore, the *HMGR* gene not only directly affects the contents of MVA-derived isoprenoids but also indirectly affects the content of MEP-derived isoprenoids by changing the expression levels of MEP-related genes.

3.5. Upregulation of MEP-derived products (ABA, GA3, and carotenoid) and MVA-derived products (TZR, IPA, DCS) in *PtDXR*-OE seedlings

The production of MEP catalyzed DXR, which is the most important rate-limiting enzyme in the MEP pathway and an important regulatory step in the cytoplasmic metabolism of isoprenoid compounds (Takahashi *et al*., 1998). In Mahmoud *et al*. (2001), overexpression of *DXR* in *Mentha piperita* promoted the synthesis of monoterpenes such as mint oil in the leaves, and increased the production of essential mint oil by 50%. In Hasunuma *et al*. (2008), overexpression of *Synechocystis sp*. strain PCC6803 *DXR* in tobacco resulted in increased levels of β-carotene, chlorophyll, antheraxanthin, and lutein. In another study, *A. thaliana DXR* mutant plants exhibited a lack of GAs, ABA, and photosynthetic pigments, and the phenotype of the mutant *A. thaliana* plants showed pale sepals and yellow inflorescences (Xing *et al*., 2010). In our study, ABA synthesis-related genes were dramatically increased, as was the accumulation of ABA, GA3, and carotenoids, in *PtDXR*-OE poplar seedlings, indicating an effect from *DXR* overexpression. Combined with the result described above of increased *DXS*, *HDS*, *HDR*, *MCT*, *CMK*, *FPS*, *GPS*, and *GPPS* expression levels, we can conclude that overexpression of *DXR* can directly affect the expression levels of MEP-related genes and that changes in MEP-related gene expression levels contribute to the yield of ABA, GA3, and carotenoids. Although the expressions of *AACT*, *HMGS*, *HMGR*, *MVK*, and *MVD*, which are related to the MVA pathway, were downregulated, the contents of the MVA-derived components TZR, IPA, and DCS were upregulated in *PtDXR*-OE seedlings, aside from their reduced CS content.

3.6. Cross-talk in the MVA and MEP pathways

Although the starting materials differ between the MVA and MEP pathways, IPP and DMAPP are common precursors. Blocking only the MVA or the MEP pathway does not completely block biosynthesis of terpenes in the cytoplasm or plastids, indicating that the common products of the MVA and MEP pathways can be transported freely to different subcellular regions (Aharoni *et al*. 2003; Aharoni *et al*. 2004; Gutensohn *et al*. 2013). For example, results of green fluorescent protein fusion and confocal microscopy have shown that

HDR is localized in the chloroplast, and the transfer of IPP from the chloroplast to cytoplasm can be observed through ^{13}C labeling, indicating that plentiful IPP is available for use in the MVA pathway to produce terpenoids (Ma *et al*. 2017). In addition, segregation between the MVA and MEP pathways is limited, and some metabolites can be exchanged on the plasmid membrane (Laule *et al*., 2003). Kim *et al*. (2016) used clustered regularly interspaced short palindromic repeats (CRISPR) technology to reconstruct the lycopene synthesis pathway and control the flow of carbon in the MEP and MVA pathways. The results showed that MVA-related genes were reduced by an average of 81.6% and the lycopene yield was significantly boosted. According to analyses of gene expression levels and metabolic yield in *PtHMGR*-OEs and *PtDXR*-OEs, we found cross-talk not only between IPP and DMAPP in the MVA and MEP pathways, but also between pairs of genes and between products of the MVA and MEP pathways in poplar cells. On one hand, overexpression of *PtDXR* affected the transcript levels of MEP-related genes and the contents of MEP-derived isoprenoids including ABA, GAs, and carotenoids. However, the decreased accumulation of MVA-related gene products reduces the yields of MVA-derived isoprenoids including CS, while increasing TZR, IPA, and DCS contents. We also found that differential expression of MVA-related genes in *PtDXR*-OE or post-transcriptional/post-translational regulation of the products of MVA-derived isoprenoids may have occurred. Furthermore, although the expression levels of MVA-related genes in *PtDXR*-OEs were lower than those in NT poplars, the transcript levels of *IDI* were upregulated in *PtDXR*-OEs, indicating that IPP and DMAPP produced by the MEP pathway could enter the cytoplasm to compensate for the lack of IPP and DMAPP there. On the other hand, *PtHMGR*-OE plants exhibited higher transcript levels of *AACT*, *MVK*, and *MVD* as well as higher expression levels of *DXS*, *DXR*, *HDS*, and *HDR* compared to NT, which indicates that PtHMGR affects both MEP- and MVA-related gene expression levels. We successfully demonstrated that manipulation of *HMGR* in the MVA pathway of poplars results in dramatically enhanced yields of ABA, GAs, and carotenoids. This result illustrates that cytosolic *HMGR* overexpression could lead to a boost in plastidial GPP- and GGPP-derived products, including ABA, GAs, and carotenoids. Therefore, this study provides evidence that cross-talk between the MVA and MEP pathways increased the expression levels of *GPS* and *GPPS* in *PtHMGR*-OEs, and elevated the contents of ABA, GA3, and carotenoids. Moreover, changes in MEP- and MVA-related gene expression levels affect MVA- and MEP-derived isoprenoids. Together, these results illustrate the phenomenon of cross-talk between the MVA

and MEP pathways. The mechanism underlying this exchange between the MVA and MEP pathways requires further research.

In conclusions, Isoprenoid compounds are diverse, with complex structures and different properties, and play an important role in the survival and growth of plants. The basic framework of the isoprenoid metabolic pathway has been explored, and many advances have been made in clarifying the molecular regulation of metabolic pathways and metabolic engineering. However, previous studies have been limited to *Arabidopsis*, tomato, and rice, and research on isoprenoid metabolism in perennial woody plants has just begun. In this study, the overexpression of *PtHMGR* in Nanlin 895 caused accumulation of MVA-derived isoprenoids as well as MEP-derived substances including ABA, GAs, carotenoids, and GRs, which are essential plant hormones regulating growth and stress responses. In *PtHMGR*-OE poplars, most MEP- and MVA-related genes associated with the biosynthesis of isoprenoid precursors were upregulated. In *PtDXR*-OE poplars, elevated contents of ABA, GAs, carotenoids, and GRs were attributed to increased expression of MEP-related genes as well as plastidial *GPP* and *GGPP*. Moreover, in both *PtDXR*-OE poplars, changes in MVA-related genes caused changes in MVA-derived isoprenoids, including the yields of CKs and BRs. Together, these results show that manipulation of *PtDXR and PtHMGR* is a novel strategy to influence poplar isoprenoids and provide a theoretical basis for cultivation of high-quality poplar.

4. Materials and Methods

4.1. Plant materials and growth conditions

Non-transgenic (NT) *P. trichocarpa* and Nanlin 895 (*Populus* × *euramericana* cv. ‘Nanlin 895’) plants were cultured in half-strength Murashige and Skoog (1/2 MS) medium (PH 5.8) under conditions of 24°C and 74% humidity. Subsequently, NT and transgenic poplars were cultured in 1/2 MS under long-day conditions (16 h light/8 h dark) at 24°C for 1 month.

4.2. *PtHMGR* gene isolation and vector construction

Total RNA was extracted from *P. trichocarpa* leaves and reverse transcriptase (TaKaRa, Japan) was used to amplify the cDNA. Forward and reverse primers (Supplemental Table: *PtHMGR*-F and *PtHMGR*-R) were designed and polymerase chain reaction (PCR) was performed to synthesize the open region frame (ORF) of the *PtHMGR* gene. Subsequently, the product of the *PtHMGR* gene was ligated into the PEASY-T3 vector (TransGen Biotech, China) based on blue-white spot screening and the *PtHMGR* gene was inserted into the vector $pGWB_9$ (Song *et al.*, 2016) using gateway technology (Invitrogen, USA).

To identify the copy number of *PtHMGR* in *P. trichocarpa*, total genomic DNA was extracted from leaves according to the cetyltrimethylammonium bromide (CTAB) method and Southern blotting was performed. The poplar DNA was digested with *Eco*RI at 37°C for 4 h and the digested poplar DNA was separated on a 0.8% agarose gel at 15 V. Then the separated poplar DNA was transferred to a Hybond N^+ nylon membrane and blotting was performed according to the manufacturer's instructions (Roche, Basel, Switzerland). The details of probe 1 and probe 2 used for Southern blotting are provided in Supplemental Table 1.

4.3. Creation of phylogenetic tree

To cluster families based on protein-coding genes, the protein data for 10 plant species were downloaded Phytozome (https://phytozome.jgi.doe.gov/pz/portal.html): *P. trichocarpa* (v3.1), *Oryza sativa* (v7), *Manihot esculenta* (v6.1), *Theobroma cacao* (v1.1), *Gossypium hirsutum* (v1.1), *Prunus persica* (v2.1), *Malus domestica* (v1.0), *Arabidopsis thaliana TAIR10*, and *Zea mays* PH207 (v1.1). Only the gene model for each gene locus that encodes the longest protein sequence was retained to remove redundant sequences. Then we employed DIAMOND software to identify potentially orthologous gene families among the filtered protein sequences of these species using a maximum e-value of 1e-5 (Buchfink *et al*., 2015). We used the OrthoFinder (v2.3.3) pipeline to identify single-copy gene families based on the aligned results with the default parameters (Emms *et al*., 2015).

We applied MAFFT (v7.158b) software (Katoh and Standley, 2013) for multiple sequence alignment of protein-coding sequences for each single-copy gene using the accurate option (LINS-i). Meanwhile, trimAl (v1.2) software (Capella-Gutiérrez *et al*., 2009) was employed to remove poorly aligned positions and divergent regions with the default parameters, and the alignments of all of the single-copy genes were concatenated to form a supermatrix. We used the program RAxML (v8.2.12) (Stamatakis, 2014) with the JTT+G+F model and 1000 bootstrap replicates to construct the supermatrix phylogenetic tree. Finally, the phylogenetic tree was visualized using FigTree (v1.4.3) (Drummond *et al*., 2009). The amino acid sequences of HMGR from *P. trichocarpa*, *M. esculenta*, *S. purpurea*, *T. cacao*, *G. hirsutum*, *D. persica*, *M. domestica*, *A. thaliana*, and *Z. mays* were obtained from the National Center for Biotechnology Information database (https://www.ncbi.nlm.nih.gov/) and Phytozome and MEGA5.0 software was used to construct a phylogenetic tree using 1000 bootstrap replicates.

4.4. Generation and characterization of transgenic poplars

Agrobacterium EHA105 containing a recombinant plasmid was used for infection of

Nanlin 895 (*Populus* × *euramericana* cv. 'Nanlin 895') leaves and petioles (Movahedi *et al*., 2015). Poplar buds were screened on differentiation MS medium amended with 30 μg/mL Kan and the resistant buds were planted in bud elongation MS medium containing 20 μg/mL Kan and transplanted into 1/2 MS medium containing 10 μg/mL Kan to generate resistant poplar trees. Subsequently, the DNA and RNA of putative transgenic poplars were isolated and analyzed via PCR and quantitative reverse transcription PCR (qRT-PCR).

4.5. Analyses via qRT-PCR

PtDXR-OE poplars have been obtained previously (Xu *et al*., 2019), and in this study we extracted RNA from 12-month-old *PtDXR*-OE and *PtHMGR*-OE poplars. qRT-PCR was performed to identify the expression levels of MVA- and MEP-related genes in NT, *PtDXR*-OE, and *PtHMGR*-OE poplars. qRT-PCR was performed with a StepOne Plus Real-time PCR System (Applied Biosystems, USA) and SYBR Green Master Mix (Roche, Germany). Poplar *Actin* (*PtActin*) (XM-006370951.1) has previously been tested as an internal control for estimating the amount of RNA in samples (Zhang *et al*., 2013). The following conditions were used for qRT-PCR reactions: pre-denaturation at 95°C for 10 min, followed by 40 cycles of denaturation at 95°C for 15 s and chain extension at 60°C for 1 min. Three independent experiments were conducted using gene-specific primers (Supplemental Table 1).

4.6. Analyses of ABA, GAs, CKs, GRs, BRs, and carotenoids via high-performance liquid chromatography tandem mass spectrometry (HPLC-MS/MS)

ABA, GAs, and CKs were extracted from NT, *PtDXR*-OE, and *PtHMGR*-OE leaves, and then HPLC-MS/MS (Qtrap6500, Agilent, USA) was used to quantitatively determine levels of ABA, GAs, zeatin, trans-zeatin-riboside (TZR), and isopentenyl adenosine (IPA). HPLC-MS/MS (Aglient1290, AB; SCIEX-6500Qtrap, Agilent; USA) was also used to determine the contents of 5-deoxystrgol (5-DS), castasterone (CS), and 6-deoxyocastasterone (DCS). In addition, the carotenoid component of poplar leaves was isolated and HPLC (Symmetry Shield RP18, Waters, USA) was used to determine the contents of carotenoids including β-carotene, lycopene, and lutein

Author contributions

Q.Z. conceived the study. H.W. and A.M. performed the experiments and carried out the analysis. H.W., A.M., C.X., W.B.S., P.W., D.W.L. and Q.Z designed the experiments and wrote the manuscript. All authors read and approved the final manuscript.

Conflict of interest

The authors declare that they have no conflict of interest.

Acknowledgments

This work was supported by the National Key Program on Transgenic Research (2018ZX08020002), the National Science Foundation of China (No. 31570650) and the Priority Academic Program Development of Jiangsu Higher Education Institutions.

Reference

Aharoni, A., Giri, A. P., Deuerlein, S., Griepink, F., de Kogel, W. J., Verstappen, F. W., ... & Bouwmeester, H. J., 2003. Terpenoid metabolism in wild-type and transgenic Arabidopsis plants. Plant Cell, 15, 2866-2884.

Aharoni, A., Giri, A. P., Verstappen, F. W., Bertea, C. M., Sevenier, R., Sun, Z., ... & Bouwmeester, H. J., 2004. Gain and loss of fruit flavor compounds produced by wild and cultivated strawberry species. Plant Cell, 16, 3110-3131.

Aharoni, A., Jongsma, M. A., & Bouwmeester, H. J., 2005. Volatile science? Metabolic engineering of terpenoids in plants. Trends Plant Sci. 10, 594-602.

Bouvier, F., Rahier, A., & Camara, B., 2005. Biogenesis, molecular regulation, and function of plant isoprenoids. Prog. Lipid Res. 44, 357-429.

Buchfink, B., Xie, C., & Huson, D. H., 2015. Fast and sensitive protein alignment using DIAMOND. Nat. Methods. 12, 59.

Capella-Gutiérrez, S., Silla-Martínez, J. M., & Gabaldón, T., 2009. trimAl: a tool for automated alignment trimming in large-scale phylogenetic analyses. Bioinformatics. 25, 1972-1973.

Carretero-Paulet, L., Cairo, A., Botella-Pavía, P., Besumbes, O., Campos, N., Boronat, A., & Rodríguez-Concepción, M., 2006. Enhanced flux through the methylerythritol 4-phosphate pathway in Arabidopsis plants overexpressing deoxyxylulose 5-phosphate reductoisomerase. Plant Mol. Biol. 62, 683-695.

Cowan, A. K., Moore-Gordon, C. S., Bertling, I., & Wolstenholme, B. N., 1997. Metabolic control of avocado fruit growth (isoprenoid growth regulators and the reaction catalyzed by 3-hydroxy-3-methylglutaryl coenzyme A reductase). Plant Physiol.114, 511-518.

Dai, Z., Cui, G., Zhou, S. F., Zhang, X., & Huang, L., 2011. Cloning and characterization of a novel 3-hydroxy-3-methylglutaryl coenzyme A reductase gene from *Salvia miltiorrhiza*, involved in diterpenoid tanshinone accumulation. J. Plant Physiol.168, 148-157.

Drummond, A. J., & Rambaut, A., 2007. BEAST: Bayesian evolutionary analysis by sampling trees. BMC Evol. Biol. 7, 214.

Dueber, J. E., Wu, G. C., Malmirchegini, G. R., Moon, T. S., Petzold, C. J., Ullal, A. V., ... & Keasling, J. D., 2009. Synthetic protein scaffolds provide modular control over metabolic flux. Nat. Biotechnol. 27, 753.

Emms, D. M., & Kelly, S., 2015. OrthoFinder: solving fundamental biases in whole genome comparisons dramatically improves orthogroup inference accuracy. Genome Biol. 16, 157.

Enfissi, E. M., Fraser, P. D., Lois, L. M., Boronat, A., Schuch, W., & Bramley, P. M., 2005. Metabolic engineering of the mevalonate and non-mevalonate isopentenyl diphosphate-forming pathways for the production of health-promoting isoprenoids in tomato. Plant Biotechnol. J. 3, 17-27.

Esteban, R., Barrutia, O., Artetxe, U., Fernández-Marín, B., Hernández, A., & García-Plazaola, J. I., 2015. Internal and external factors affecting photosynthetic pigment composition in plants: a meta-analytical approach. New Phytol. 206, 268-280.

Ferrero, S., Grados-Torrez, R. E., Leivar, P., Antolín-Llovera, M., López-Iglesias, C., Cortadellas, N., ... & Campos, N., 2015. Proliferation and morphogenesis of the endoplasmic reticulum driven by the membrane domain of 3-hydroxy-3-methylglutaryl coenzyme A reductase in plant cells. Plant Physiol. 168, 899-914.

Gutensohn, M., Orlova, I., Nguyen, T. T., Davidovich□Rikanati, R., Ferruzzi, M. G., Sitrit, Y., ... & Dudareva, N., 2013. Cytosolic monoterpene biosynthesis is supported by plastid-generated geranyl diphosphate substrate in transgenic tomato fruits. Plant J. 75, 351-363.

Hain, Rüdiger, Reif, H. J., Krause, E., Langebartels, R., Kindl, H., & Vornam, B., et al., 1993. Disease resistance results from foreign phytoalexin expression in a novel plant. Nature, 361, 153-156.

Hasunuma, T., Takeno, S., Hayashi, S., Sendai, M., Bamba, T., Yoshimura, S., ... & Miyake, C., 2008. Overexpression of 1-deoxy-D-xylulose-5-phosphate reductoisomerase gene in chloroplast contributes to increment of isoprenoid production. J. Biosci. Bioeng. 105, 518-526.

Hemmerlin, A., Gerber, E., Feldtrauer, J. F., Wentzinger, L., Hartmann, M. A., Tritsch, D., ... & Bach, T. J., 2004. A review of tobacco BY-2 cells as an excellent system to study the synthesis and function of sterols and other isoprenoids. Lipids. 39, 723-735.

Hemmerlin, A., Harwood, J. L., & Bach, T. J., 2012. A raison d'être for two distinct pathways in the early steps of plant isoprenoid biosynthesis? Prog. Lipid Res. 51, 95-148.

Henriquez, M. A., Soliman, A., Li, G., Hannoufa, A., Ayele, B. T., & Daayf, F., 2016.

Molecular cloning, functional characterization and expression of potato (*Solanum tuberosum*) 1-deoxy-d-xylulose 5-phosphate synthase 1 (StDXS1) in response to *Phytophthora infestans*. Plant Sci. 243, 71-83.

Henry, L. K., Gutensohn, M., Thomas, S. T., Noel, J. P., & Dudareva, N., 2015. Orthologs of the archaeal isopentenyl phosphate kinase regulate terpenoid production in plants. Proc. Natl. Acad. Sci. U. S. A. 112, 10050-10055.

Huang, Z., & Szoka Jr, F. C., 2008. Sterol-modified phospholipids: cholesterol and phospholipid chimeras with improved biomembrane properties. J. Am. Chem. Soc. 130, 15702-15712.

Huchelmann, A., Gastaldo, C., Veinante, M., Zeng, Y., Heintz, D., Tritsch, D., ... & Hemmerlin, A., 2014. S-Carvone suppresses cellulase-induced capsidiol production in *Nicotiana tabacum* by interfering with protein isoprenylation. Plant Physiol. 164, 935-950.

Kai, G., Xu, H., Zhou, C., Liao, P., Xiao, J., Luo, X., ... & Zhang, L., 2011. Metabolic engineering tanshinone biosynthetic pathway in *Salvia miltiorrhiza* hairy root cultures. Metab. Eng. 13, 319-327.

Kazan, K., 2015. Diverse roles of jasmonates and ethylene in abiotic stress tolerance. Trends Plant Sci. 20, 219-229.

Kim, S. K., Han, G. H., Seong, W., Kim, H., Kim, S. W., Lee, D. H., & Lee, S. G., 2016. CRISPR interference-guided balancing of a biosynthetic mevalonate pathway increases terpenoid production. Metab. Eng. 38, 228-240.

Kim, M. S., Haney, M. J., Zhao, Y., Mahajan, V., Deygen, I., Klyachko, N. L., ... & Hingtgen, S. D., 2016. Development of exosome-encapsulated paclitaxel to overcome MDR in cancer cells. Nanomedicine. 12, 655-664.

Kim, Y. J., Lee, O. R., Ji, Y. O., Jang, M. G., & Yang, D. C., 2014. Functional analysis of HMGR encoding genes in triterpene saponin-producing *Panax ginseng* Meyer. Plant Physiol. 165, 373-387.

Kirby, J., & Keasling, J. D., 2009. Biosynthesis of plant isoprenoids: perspectives for microbial engineering. Annu. Rev. Plant Biol. 60, 335-355.

Kong, L. Y., & Tan, R. X., 2015. Artemisinin, a miracle of traditional Chinese medicine. Nat. Prod. Rep. 32, 1617-1621.

Laule, O., Fürholz, A., Chang, H. S., Zhu, T., Wang, X., Heifetz, P. B., ... & Lange, M., 2003. Crosstalk between cytosolic and plastidial pathways of isoprenoid biosynthesis in *Arabidopsis*

thaliana. Proc. Natl. Acad. Sci. U. S. A. 100, 6866-6871.

Li, W., Liu, W., Wei, H., He, Q., Chen, J., Zhang, B., & Zhu, S., 2014. Species-specific expansion and molecular evolution of the 3-hydroxy-3-methylglutaryl coenzyme A reductase (HMGR) gene family in plants. PloS One. 9, e94172.

Liao, P., Chen, X., Wang, M., Bach, T. J., & Chye, M. L., 2018. Improved fruit α-tocopherol, carotenoid, squalene and phytosterol contents through manipulation of Brassica juncea 3-HYDROXY-3-METHYLGLUTARYL-COA SYNTHASE 1 in transgenic tomato. Plant Biotechnol. J. 16, 784-796.

Liao, P., Hemmerlin, A., Bach, T. J., & Chye, M. L., 2016. The potential of the mevalonate pathway for enhanced isoprenoid production. Biotechnol. Adv. 34, 697-713.

Liao, Z. H., Chen, M., Gong, Y. F., Miao, Z. Q., Sun, X. F., & Tang, K. X., 2006. Isoprenoid biosynthesis in plants: pathways, genes, regulation and metabolic engineering. J Biol Sci. 6, 209-219.

Lu, X. M., Hu, X. J., Zhao, Y. Z., Song, W. B., Zhang, M., Chen, Z. L., ... & Lai, J. S., 2012. Map-based cloning of zb7 encoding an IPP and DMAPP synthase in the MEP pathway of maize. Mol. Plant. 5, 1100-1112.

Ma, D., Li, G., Zhu, Y., & Xie, D. Y., 2017. Overexpression and suppression of Artemisia annua 4-hydroxy-3-methylbut-2-enyl diphosphate reductase 1 gene (*AaHDR1*) differentially regulate artemisinin and terpenoid biosynthesis. Front Plant Sci. 8, 77.

Ma, Y., Yuan, L., Wu, B., Li, X. E., Chen, S., & Lu, S., 2012. Genome-wide identification and characterization of novel genes involved in terpenoid biosynthesis in *Salvia miltiorrhiza*. J. Exp. Bot. 63, 2809-2823.

Mahmoud, S. S., & Croteau, R. B., 2001. Metabolic engineering of essential oil yield and composition in mint by altering expression of deoxyxylulose phosphate reductoisomerase and menthofuran synthase. Proc. Natl. Acad. Sci. U. S. A. 98, 8915-8920.

Merret, R., Cirioni, J. R., Bach, T. J., & Hemmerlin, A., 2007. A serine involved in actin-dependent subcellular localization of a stress-induced tobacco BY-2 hydroxymethylglutaryl-CoA reductase isoform. FEBS Lett. 581, 5295-5299.

Movahedi, A., Zhang, J., Gao, P., Yang, Y., Wang, L., & Yin, T., et al., 2015. Expression of the chickpea *CarNAC3*, gene enhances salinity and drought tolerance in transgenic poplars. Plant Cell, Tissue Organ Cult. 120, 141-154.

Muñoz-Bertomeu, J., Sales, E., Ros, R., Arrillaga, I., & Segura, J., 2007. Up-regulation of an

N-terminal truncated 3-hydroxy-3-methylglutaryl CoA reductase enhances production of essential oils and sterols in transgenic *Lavandula latifolia*. Plant Biotechnol. J. 5, 746-758.

Rahman, L., Kouno, H., Hashiguchi, Y., Yamamoto, H., Narbad, A., Parr, A., ... & Kitamura, Y., 2009. HCHL expression in hairy roots of *Beta vulgaris* yields a high accumulation of p-hydroxybenzoic acid (pHBA) glucose ester, and linkage of pHBA into cell walls. Bioresour. Technol. 100, 4836-4842.

Roberts, S. C. Production and engineering of terpenoids in plant cell culture., 2007. Nat. Chem. Biol. 3, 387.

Ren, D., Liu, Y., Yang, K. Y., Han, L., Mao, G., Glazebrook, J., & Zhang, S. A fungal-responsive MAPK cascade regulates phytoalexin biosynthesis in Arabidopsis., 2008. Proc. Natl. Acad. Sci. U. S. A. 105, 5638-5643.

Rui, X., Caiqin, L., Wangjin, L., Juan, D., Zehuai, W., & Jianguo, L., 2012. 3-Hydroxy-3-methylglutaryl coenzyme A reductase 1 (HMG1) is highly associated with the cell division during the early stage of fruit development which determines the final fruit size in *Litchi chinensis*. Gene. 498, 28-35.

Schaller, H., Grausem, B., Benveniste, P., Chye, M. L., Tan, C. T., Song, Y. H., & Chua, N. H., 1995. Expression of the *Hevea brasiliensis* (HBK) Mull. Arg. 3-hydroxy-3-methylglutaryl-coenzyme A reductase 1 in tobacco results in sterol overproduction. Plant Physiol. 109, 761-770.

Schie, C. C. V. Haring, M. A., Schuurink, R. C., 2006. Regulation of terpenoid and benzenoid production in flowers. Curr. Opin. Plant Biol. 9, 203-208.

Simpson, K., Quiroz, L. F., Rodriguez-Concepción, M., & Stange, C. R., 2016. Differential contribution of the first two enzymes of the MEP pathway to the supply of metabolic precursors for carotenoid and chlorophyll biosynthesis in carrot (*Daucus carota*). *Front Plant Sci*. 7, 1344.

Song, X., Yu, X., Hori, C., Demura, T., Ohtani, M., & Zhuge, Q., 2016. Heterologous overexpression of poplar *SnRK2* genes enhanced salt stress tolerance in *Arabidopsis thaliana*. Front Plant Sci. 7, 612.

Stamatakis, A., 2014. RAxML version 8: a tool for phylogenetic analysis and post-analysis of large phylogenies. Bioinformatics. 30, 1312-1313.

Suzuki, M., Kamide, Y., Nagata, N., Seki, H., Ohyama, K., & Kato, H., et al., 2005. Loss of function of 3-hydroxy-3-methylglutaryl coenzyme A reductase 1 (HMGR1) in *Arabidopsis*

leads to dwarfing, early senescence and male sterility, and reduced sterol levels. Plant J. 20, 67-77.

Takahashi, S., Kuzuyama, T., Watanabe, H., & Seto, H., 1998. A 1-deoxy-D-xylulose 5-phosphate reductoisomerase catalyzing the formation of 2-C-methyl-D-erythritol 4-phosphate in an alternative nonmevalonate pathway for terpenoid biosynthesis. Proc. Natl. Acad. Sci. U. S. A. 95, 9879-9884.

Tiski, I., Marraccini, P., Pot, D., Vieira, L. G. E., & Pereira, L. F. P., 2011. Characterization and expression of two cDNA encoding 3-Hydroxy-3-methylglutaryl coenzyme A reductase isoforms in coffee (*Coffea arabica L.*). OMICS: J. Integr. Biol. 15, 719-727.

Vaccaro, M., Malafronte, N., Alfieri, M., De Tommasi, N., & Leone, A., 2014. Enhanced biosynthesis of bioactive abietane diterpenes by overexpressing *AtDXS* or *AtDXR* genes in *Salvia sclarea* hairy roots. Plant Cell, Tissue Organ Cult. 119, 65-77.

Wang, H., Nagegowda, D. A., Rawat, R., Bouvier-Navé, P., Guo, D., Bach, T. J., & Chye, M. L., 2012. Overexpression of Brassica juncea wild-type and mutant HMG-CoA synthase 1 in Arabidopsis up-regulates genes in sterol biosynthesis and enhances sterol production and stress tolerance. Plant Biotechnol. J. 10, 31-42.

Weber, P., Bendich, A., & Machlin, L. J., 1997. Vitamin E and human health: rationale for determining recommended intake levels. Nutrition. 13, 450-460.

Wong, C. W., Czarny, B., Metselaar, J. M., Ho, C., Ng, S. R., Barathi, A. V., ... & Wong, T. T., 2018. Evaluation of subconjunctival liposomal steroids for the treatment of experimental uveitis. Sci. Rep. 8, 6604.

Xie, Z., Kapteyn, J., & Gang, D. R., 2008. A systems biology investigation of the MEP/terpenoid and shikimate/phenylpropanoid pathways points to multiple levels of metabolic control in sweet basil glandular trichomes. Plant J. 54, 349-361.

Xing, S., Miao, J., Li, S., Qin, G., Tang, S., Li, H., ... & Qu, L. J., 2010. Disruption of the 1-deoxy-D-xylulose-5-phosphate reductoisomerase (*DXR*) gene results in albino, dwarf and defects in trichome initiation and stomata closure in Arabidopsis. Cell Res. 20, 688.

Xu, C., Wei, H., Movahedi, A., Sun, W., Ma, X., Li, D., ... & Zhuge, Q., 2019. Evaluation, characterization, expression profiling, and functional analysis of *DXS* and *DXR* genes of *Populus trichocarpa*. Plant Physiol. Biochem. 142.

Xu, J. W., Xu, Y. N., & Zhong, J. J., 2012. Enhancement of ganoderic acid accumulation by overexpression of an N-terminally truncated 3-hydroxy-3-methylglutaryl coenzyme A

reductase gene in the basidiomycete *Ganoderma lucidum*. Appl. Environ. Microbiol. 78, 7968-7976.

Yamaguchi, S., Kamiya, Y., & Nambara, E., 2018. Regulation of ABA and GA levels during seed development and germination in Arabidopsis. Annu. Plant Rev. 27, 224-247.

Zhang, K., Fan, W., Huang, Z., Chen, D., Yao, Z., Li, Y., ... & Qiu, D., 2019. Transcriptome analysis identifies novel responses and potential regulatory genes involved in 12-deoxyphorbol-13-phenylacetate biosynthesis of *Euphorbia resinifera*. Ind. Crops Prod. 135, 138-145.

Zhang, H., Niu, D., Wang, J., Zhang, S., Yang, Y., Jia, H., & Cui, H., 2015. Engineering a platform for photosynthetic pigment, hormone and cembrane-related diterpenoid production in *Nicotiana tabacum*. Plant Cell Physiol. 56, 2125-2138.

Zhang, J., Li, J., Liu, B., Zhang, L., Chen, J., & Lu, M., 2013. Genome-wide analysis of the *populus* hsp90 gene family reveals differential expression patterns, localization, and heat stress responses. BMC Genomics. 14.

Zhang, L., Ding, R., Chai, Y., Bonfill, M., Moyano, E., Oksman-Caldentey, K. M., ... & Kai, G., 2004. Engineering tropane biosynthetic pathway in *Hyoscyamus niger* hairy root cultures. Proc. Natl. Acad. Sci. U. S. A. 101, 6786-6791.

Zhang, Y., Zhao, Y., Wang, J., Hu, T., Tong, Y., Zhou, J., ... & Huang, L., 2018. Overexpression and RNA interference of *TwDXR* regulate the accumulation of terpenoid active ingredients in *Tripterygium wilfordii*. Biotechnol. Lett. 40, 419-425.

Figure legends

Figure 1. Southern blotting analyses of homologous *PtHMGR* copy number and identification of probes specific to *PtHMGR* (Potri.004G208500.1). (A) Southern blotting was performed to determine the copy number of homologous *PtHMGR* genes using probe 1. (B) Southern blotting was performed using probe 2 to specifically recognize *PtHMGR* (Potri.004G208500.1).

Figure 2. Phylogenetic analyses. (A) Construction of a phylogenetic tree based on the whole genomes of various species. (B) Construction of a phylogenetic tree based on the HMGR sequences of various species. Accession numbers of the HMGR obtained from GenBank are as

follows: *Arabidopsis thaliana* (NP_177775.2), *Gossypium hirsutum* (XP_016691783.1), *Malus domestica* (XP_008348952.1), *Manihot esculenta* (XP_021608133.1), *Prunus persica* (XM_020569919.1), *Oryza sativa* (XM_015768351.2), *Theobroma cacao* (XM_007043046.2), *Zea mays* (PWZ28886.1).

Figure 3. qRT-PCR analyses of the transcript levels of MEP- and MVA-related genes in *PtHMGR-OE*s. Transcript levels of MEP-related genes including *DXS*, *DXR*, *MCT*, *CMK*, *HDS*, and HDR; of MVA-related genes including *AACT*, *HMGS*, *MVK*, and *MVD*; and of downstream genes including *IDI*, *GPS*, *GPPS*, and *GGPPS*. *PtActin* was used as an internal reference. Vertical bars represent mean ± SD (n = 3). *significant difference between *HMGR*-OEs and NT poplars at P < 0.05. **significant difference between *HMGR*-OEs and NT poplars at P < 0.01. ***significant difference between *HMGR*-OEs and NT poplars at P < 0.001.

Figure 4. qRT-PCR analyses of transcript levels of MEP- and MVA-related genes in *PtDXR*-OEs. Transcript levels of MEP-related genes including *DXS*, *MCT*, *CMK*, *HDS*, and HDR; of MVA-related genes including *AACT*, *HMGS*, *HMGR*, *MVK*, and *MVD*; and of downstream genes including *IDI*, *GPS*, *GPPS*, and *GGPPS*. *PtActin* was used as an internal reference. Vertical bars represent mean ± SD (n = 3). *significant difference between *DXR-OE*s and NT poplars at P < 0.05. **significant difference between *PtDXR*-OEs and NT poplars at P < 0.01. ***significant difference between *PtDXR*-OEs and NT poplars at P < 0.001.

Figure 5. qRT-PCR analyses of the expression levels of ABA synthesis-related genes and HPLC-MS/MS analyses of the contents of ABA, β-carotene, lycopene and lutein in *PtHMGR*-OEs. The expression levels of ABA synthesis-related genes including *NCED1*, *NCED3*, *NCED5*, *NCED6*, *ZEP1*, *ZEP2*, and *ZEP3* are shown. Vertical bars represent mean ± SD (n = 3). *significant difference at P < 0.05. **significant difference at P < 0.01. ***significant difference at P < 0.001. Three independent experiments were performed in this study.

Figure 6. HPLC-MS/MS analyses of the contents of GA3 (A), TZR (B), IPA(C), DCS (D), and CS (E) in *PtHMGR*-OEs and NT poplars.

Figure 7. qRT-PCR analyses of the expression levels of ABA synthesis-related genes and HPLC-MS/MS analyses of the contents of ABA, β-carotene, lycopene and lutein in *PtDXR*-OEs and NT poplars. The expression levels of ABA synthesis related genes including *NCED1*, *NCED3*, *NCED5*, *NCED6*, *ZEP1*, *ZEP2*, and *ZEP3* are shown. Vertical bars represent

mean ± SD (n = 3). *significant difference at P < 0.05. **significant difference at P < 0.01. ***significant difference at P < 0.001. Three independent experiments were performed in this study.

Figure 8. HPLC-MS/MS analyses of the contents of GA3 (A), TZR (B), IPA(C), DCS (D), and CS (E) in *PtDXR*-OEs and NT poplars.

Supplementary Figures

Supplemental Figure 1. Amino acid sequences alignment of PtHMGR protein and other known HMGR proteins. *A. thaliana* (NP_177775.2), *G. hirsutum* (XP_016691783.1), *M. domestica* (XP_008348952.1), *M. esculenta* (XP_021608133.1), *P. persica* (XM_020569919.1), *O. sativa* (XM_015768351.2), *T. cacao* (XM_007043046.2), *Z. mays* (PWZ28886.1).

Supplemental Figure 2. Molecular identification of *PtHMGR*-OEs. (A) Identification of *PtHMGR* in *PtHMGR*-OEs and NT poplars based on the results of PCR. (B) Identification of the transcript levels of *PtHMGR* in *PtHMGR*-OEs and NT poplars based on the results of qRT-PCR. Three independent experiments were performed. *significant difference at P < 0.05. **significant difference at P < 0.01. ***significant difference at P < 0.001.

Supplemental Figure 3. Analyses of the chromatogram of ABA standards via HPLC-MS/MS. The chromatogram of standard ABA at (A) 0.1, (B) 0.2, (C) 0.5, (D) 2, (E) 5, (F) 20, (G) 50, and (H) 200 ng/mL concentrations. (I) Equations for the ABA standard curves.

Supplemental Figure 4. Analyses of the chromatogram of GA1 standards via HPLC-MS/MS. The chromatogram of standard GA1 at (A) 0.1, (B) 0.2, (C) 0.5, (D) 2, (E) 5, (F) 20, (G) 50, and (H) 200 ng/mL concentrations. (I) Equations for the GA1 standard curves.

Supplemental Figure 5. Analyses of the chromatogram of GA3 standards via HPLC-MS/MS. The chromatogram of standard GA3 at (A) 0.1, (B) 0.2, (C) 0.5, (D) 2, (E) 5, (F) 20, (G) 50, and (H) 200 ng/mL concentrations. (I) Equations for the GA3 standard curves.

Supplemental Figure 6. Analyses of the chromatogram of GA4 standards via HPLC-MS/MS. The chromatogram of standard GA4 at (A) 0.2, (B) 0.5, (C) 2, (D) 5, (E) 20, (F) 50, and (G) 200 ng/mL concentrations. (H) Equations for the GA4 standard curves.

Supplemental Figure 7. Analyses of the chromatogram of GA7 standards via HPLC-MS/MS. The chromatogram of standard GA7 at (A) 0.1, (B) 0.5, (C) 2, (D) 5, (E) 20, (F) 50, and (G) 200 ng/mL concentrations. (H) Equations for the GA7 standard curves.

Supplemental Figure 8. Analyses of the chromatogram of zeatin standards via HPLC-MS/MS.

The chromatogram of standard zeatin at (A) 0.5, (B) 1, (C) 2, (D) 5, (E) 20, (F) 50, and (G) 200 ng/mL concentrations. (H) Equations for the zeatin standard curves.

Supplemental Figure 9. Analyses of the chromatogram of TZR standards via HPLC-MS/MS. The chromatogram of standard TZR at (A) 0.1, (B) 0.2, (C) 0.5, (D) 2, (E) 5, (F) 20, (G) 50, and (H) 200 ng/mL concentrations. (I) Equations for the TZR standard curves.

Supplemental Figure 10. Analyses of the chromatogram of IP standards via HPLC-MS/MS. The chromatogram of standard IP at (A) 0.1, (B) 2, (C) 5, (D) 20, (E) 50, and (F) 200 ng/mL concentrations. (G) Equations for the IP standard curves.

Supplemental Figure 11. Analyses of the chromatogram of IPA standards via HPLC-MS/MS. The chromatogram of standard IPA at (A) 0.2, (B) 0.5, (C) 2, (D) 5, (E) 20, (F) 50, and (G) 200 ng/mL concentrations. (H) Equations for the IPA standard curves.

Supplemental Figure 12. Analyses of the chromatogram of CS standards via HPLC-MS/MS. The chromatogram of standard CS at (A) 0.5, (B) 5, (C) 10, (D) 20, and (E) ng/mL concentrations. (F) Equations for the CS standard curves.

Supplemental Figure 13. Analyses of the chromatogram of DCS standards via HPLC-MS/MS. The chromatogram of standard DCS at (A) 0.5, (B) 2, (C) 10, (D) 50, and (E) ng/mL concentrations. (F) Equations for the DCS standard curves.

Supplemental Figure 14. HPLC-MS/MS analyses of the contents of zeatin (A), IP (B), GA1 (C), GA4 (D), and GA7 (E) in *PtHMGR*-OEs and NT poplars.

Supplemental Figure 15. HPLC-MS/MS analyses of the contents of zeatin (A), IP (B), GA1 (C), GA4 (D), and GA7 (E) in *PtDXR*-OEs and NT poplars.

Table legends

Primers used in this study.

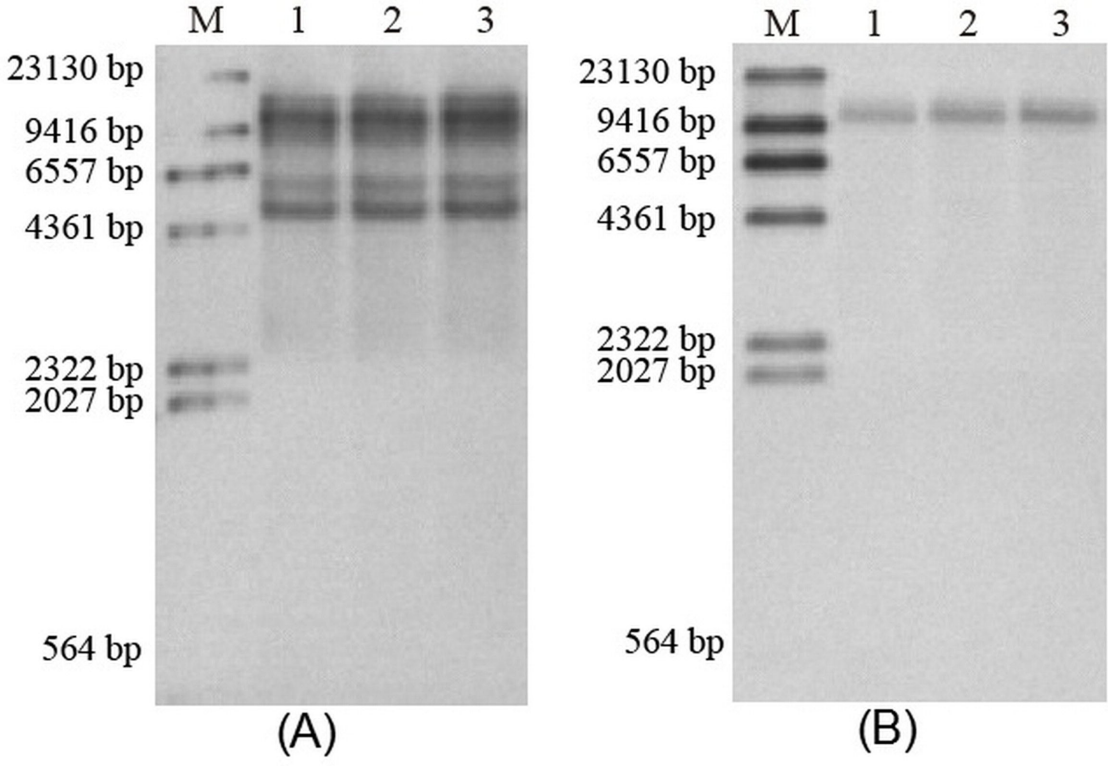
M
1
2
3
23130 bp
9416 bp
6557 bp
4361 bp
2322 bp
2027 bp
564 bp
(A)
M
1
2
3
23130 bp
9416 bp
6557 bp
4361 bp
2322 bp
2027 bp
564 bp
(B)

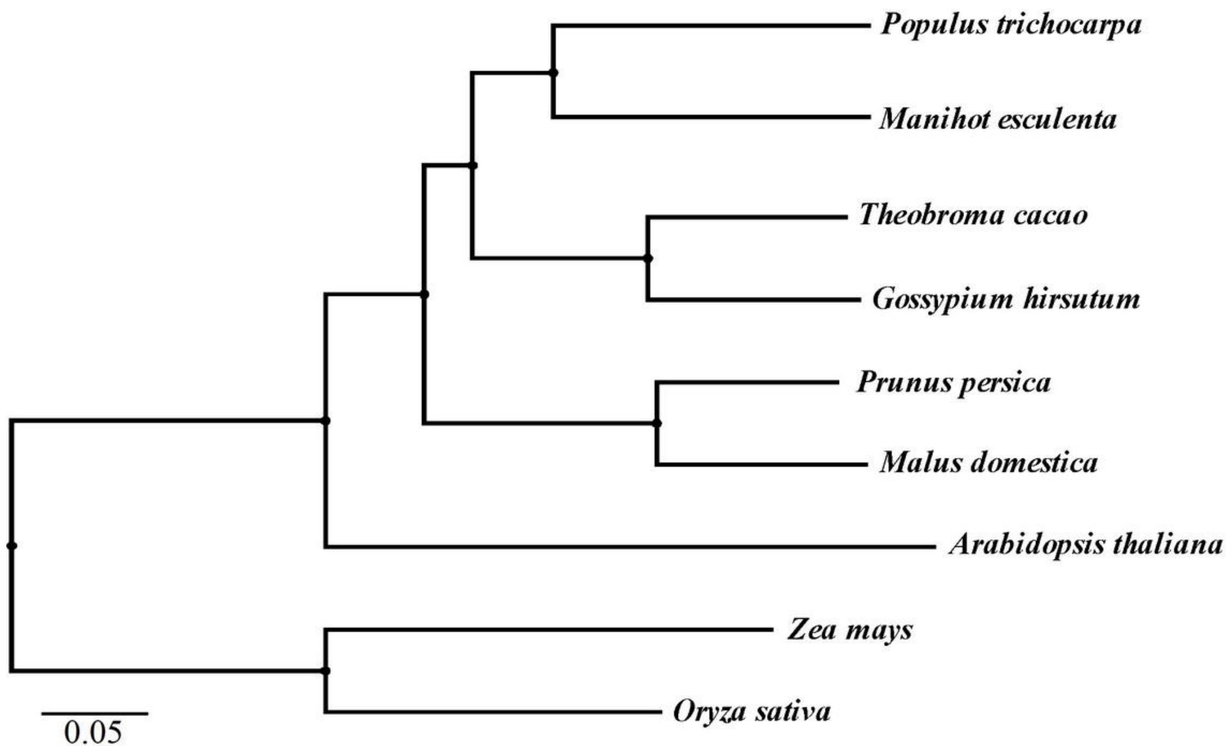
Populus trichocarpa
Manihot esculenta
Theobroma cacao
Gossypium hirsutum
Prunus persica
Malus domestica
Arabidopsis thaliana
Zea mays
Oryza sativa
0.05

(A)

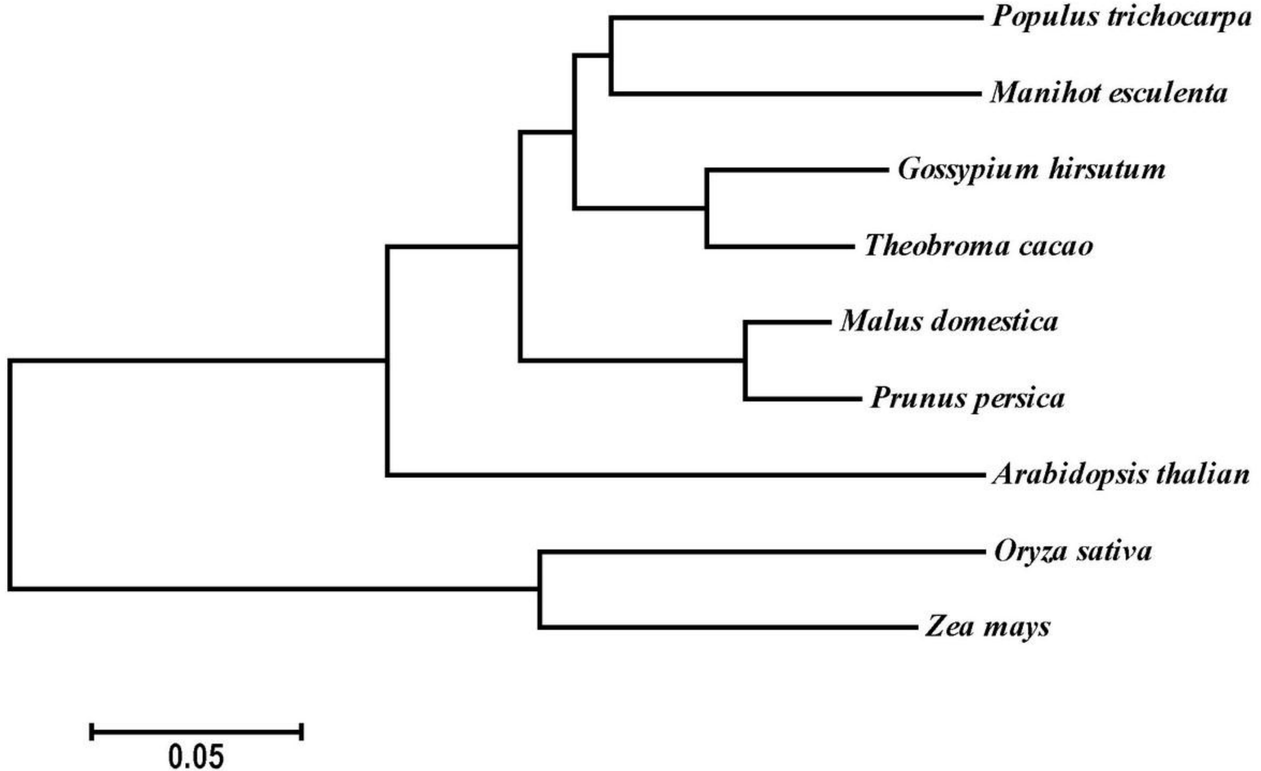
Populus trichocarpa
Manihot esculenta
Gossypium hirsutum
Theobroma cacao
Malus domestica
Prunus persica
Arabidopsis thalian
Oryza sativa
Zea mays
0.05

(B)

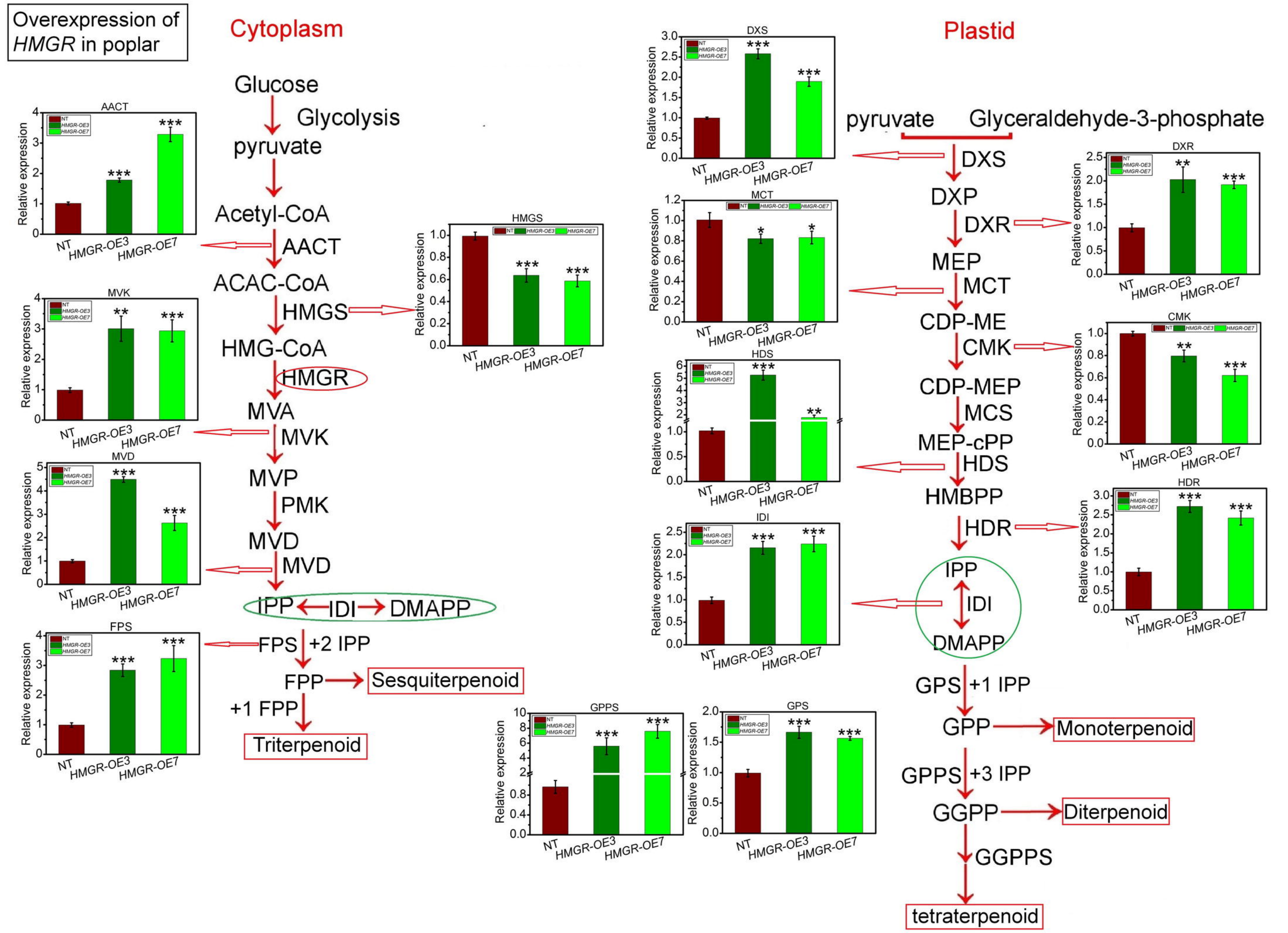
Overexpression of HMGR in poplar
Cytoplasm
Glucose
Glycolysis
pyruvate
Acetyl-CoA
AACT
ACAC-CoA
HMGS
HMG-CoA
HMGR
MVA
MVK
MVP
PMK
MVD
MVD
IPP
IDI
DMAPP
FPS
+2 IPP
FPP
Sesquiterpenoid
+1 FPP
Triterpenoid
Plastid
pyruvate
Glyceraldehyde-3-phosphate
DXS
DXP
DXR
MEP
MCT
CDP-ME
CMK
CDP-MEP
MCS
MEP-cPP
HDS
HMBPP
HDR
IPP
IDI
DMAPP
GPS
+1 IPP
GPP
Monoterpenoid
GPPS
+3 IPP
GGPP
Diterpenoid
GGPPS
tetraterpenoid
AACT
MVK
MVD
FPS
HMGS
DXS
MCT
HDS
IDI
GPPS
GPS
DXR
CMK
HDR
Relative expression
NT
HMGR-OE3
HMGR-OE7

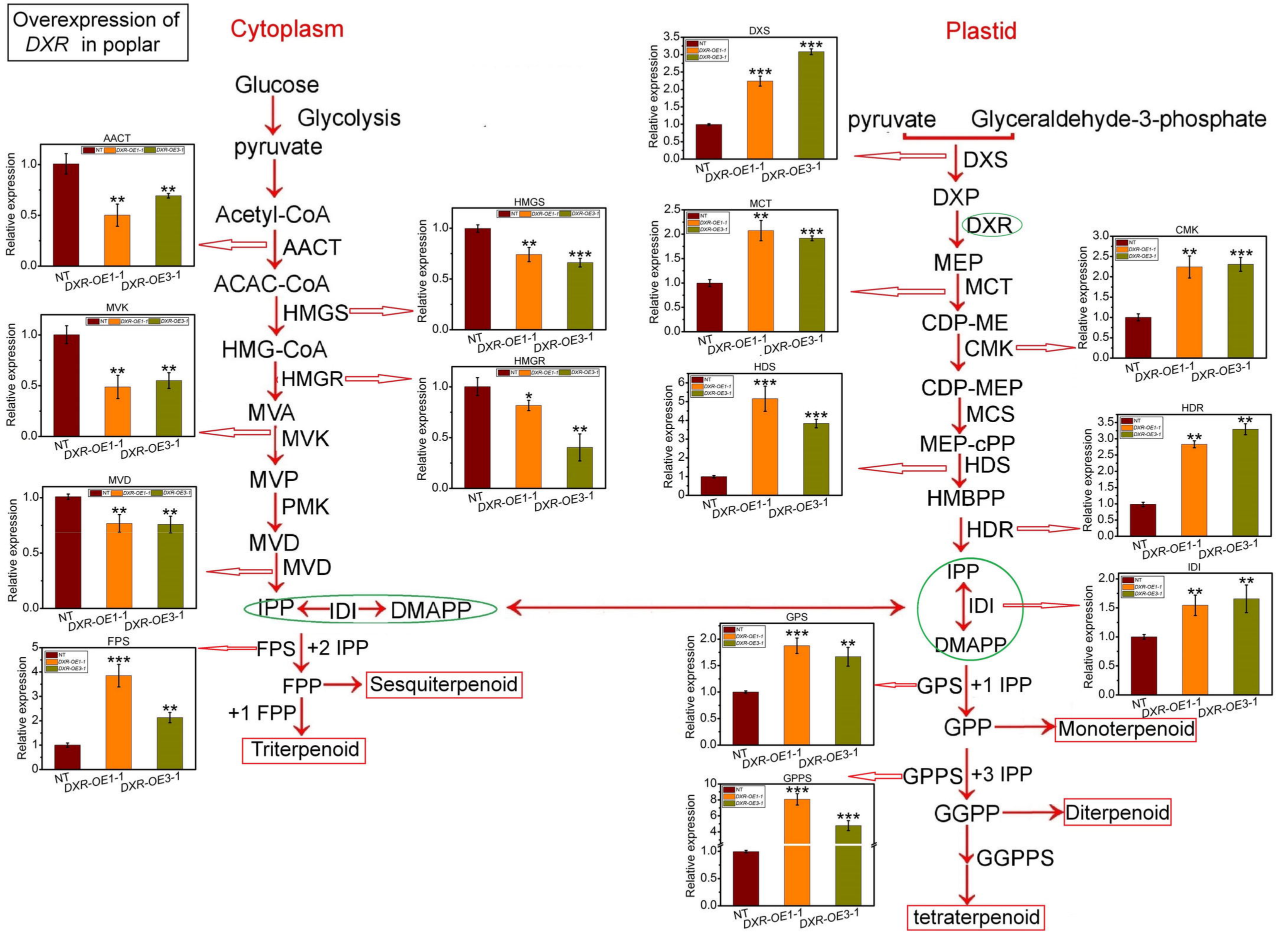
Overexpression of DXR in poplar
Cytoplasm
Plastid
Glucose
Glycolysis
pyruvate
Acetyl-CoA
AACT
ACAC-CoA
HMGS
HMG-CoA
HMGR
MVA
MVK
MVP
PMK
MVD
MVD
IPP
IDI
DMAPP
FPS
+2 IPP
FPP
Sesquiterpenoid
+1 FPP
Triterpenoid
pyruvate
Glyceraldehyde-3-phosphate
DXS
DXP
DXR
MEP
MCT
CDP-ME
CMK
CDP-MEP
MCS
MEP-cPP
HDS
HMBPP
HDR
IPP
IDI
DMAPP
GPS
+1 IPP
GPP
Monoterpenoid
GPPS
+3 IPP
GGPP
Diterpenoid
GGPPS
tetraterpenoid
AACT
MVK
MVD
FPS
HMGS
HMGR
DXS
MCT
HDS
CMK
HDR
IDI
GPS
GPPS
NT
DXR-OE1-1
DXR-OE3-1
Relative expression

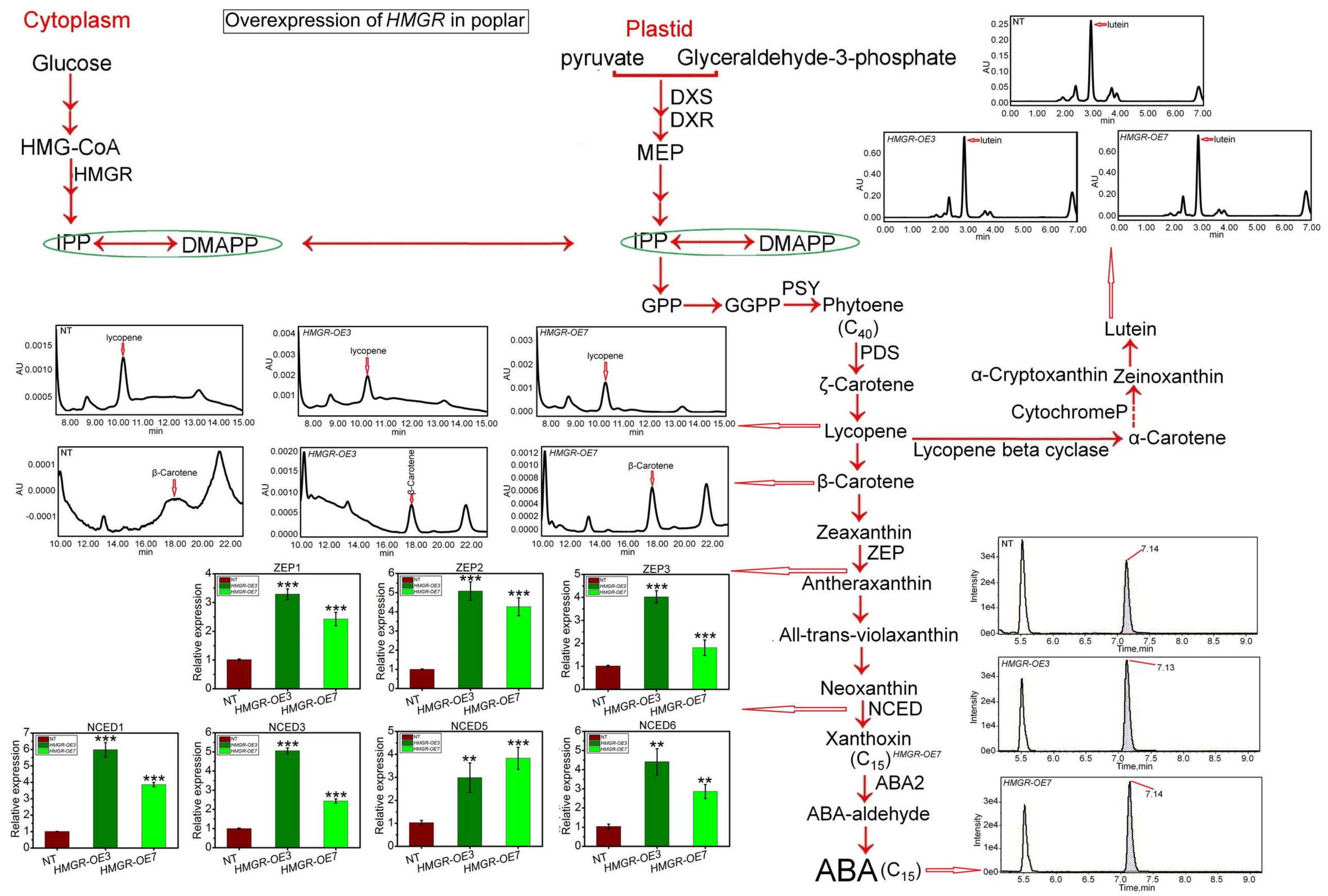
Cytoplasm
Overexpression of HMGR in poplar
Plastid
Glucose
HMG-CoA
HMGR
IPP
DMAPP
pyruvate
Glyceraldehyde-3-phosphate
DXS
DXR
MEP
IPP
DMAPP
GPP
GGPP
PSY
Phytoene
(C40)
PDS
ζ-Carotene
Lycopene
Lycopene beta cyclase
α-Carotene
CytochromeP
α-Cryptoxanthin
Zeinoxanthin
Lutein
β-Carotene
Zeaxanthin
ZEP
Antheraxanthin
All-trans-violaxanthin
Neoxanthin
NCED
Xanthoxin
(C15)
HMGR-OE7
ABA2
ABA-aldehyde
ABA(C15)
NT
HMGR-OE3
HMGR-OE7
lycopene
β-Carotene
lutein
AU
min
ZEP1
ZEP2
ZEP3
NCED1
NCED3
NCED5
NCED6
Relative expression
Intensity
Time,min
7.14
7.13

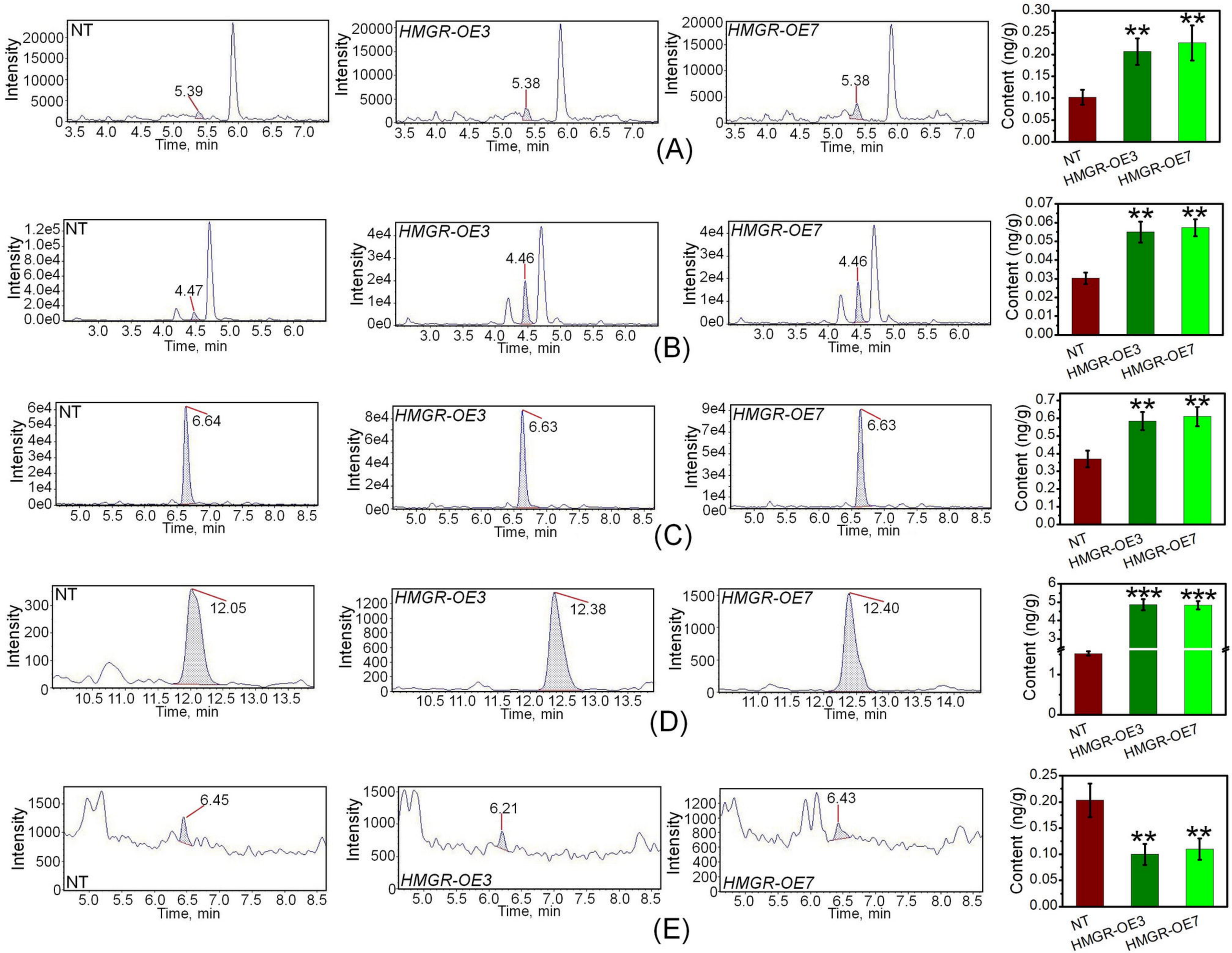
NT
HMGR-OE3
HMGR-OE7
Intensity
Time, min
5.39
5.38
5.38
Content (ng/g)
**
**
(A)
4.47
4.46
4.46
(B)
6.64
6.63
6.63
(C)
12.05
12.38
12.40
***
***
(D)
6.45
6.21
6.43
(E)

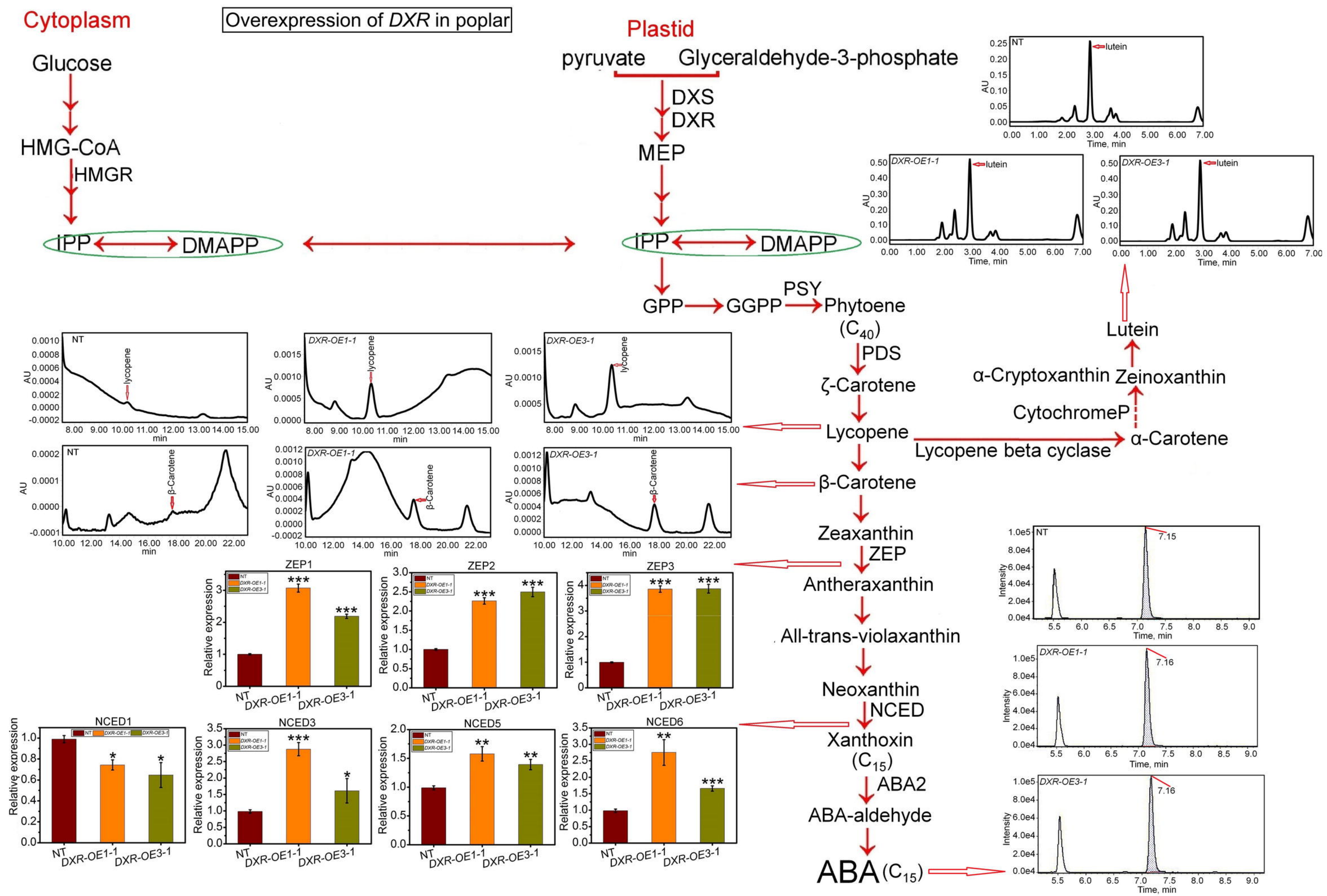
Cytoplasm
Overexpression of DXR in poplar
Plastid
Glucose
HMG-CoA
HMGR
IPP
DMAPP
pyruvate
Glyceraldehyde-3-phosphate
DXS
DXR
MEP
IPP
DMAPP
GPP
GGPP
PSY
Phytoene
(C40)
PDS
ζ-Carotene
Lycopene
Lycopene beta cyclase
α-Carotene
CytochromeP
α-Cryptoxanthin
Zeinoxanthin
Lutein
β-Carotene
Zeaxanthin
ZEP
Antheraxanthin
All-trans-violaxanthin
Neoxanthin
NCED
Xanthoxin
(C15)
ABA2
ABA-aldehyde
ABA (C15)
NT
DXR-OE1-1
DXR-OE3-1
lutein
lycopene
β-Carotene
AU
min
Time, min
Intensity
7.15
7.16
ZEP1
ZEP2
ZEP3
NCED1
NCED3
NCED5
NCED6
Relative expression

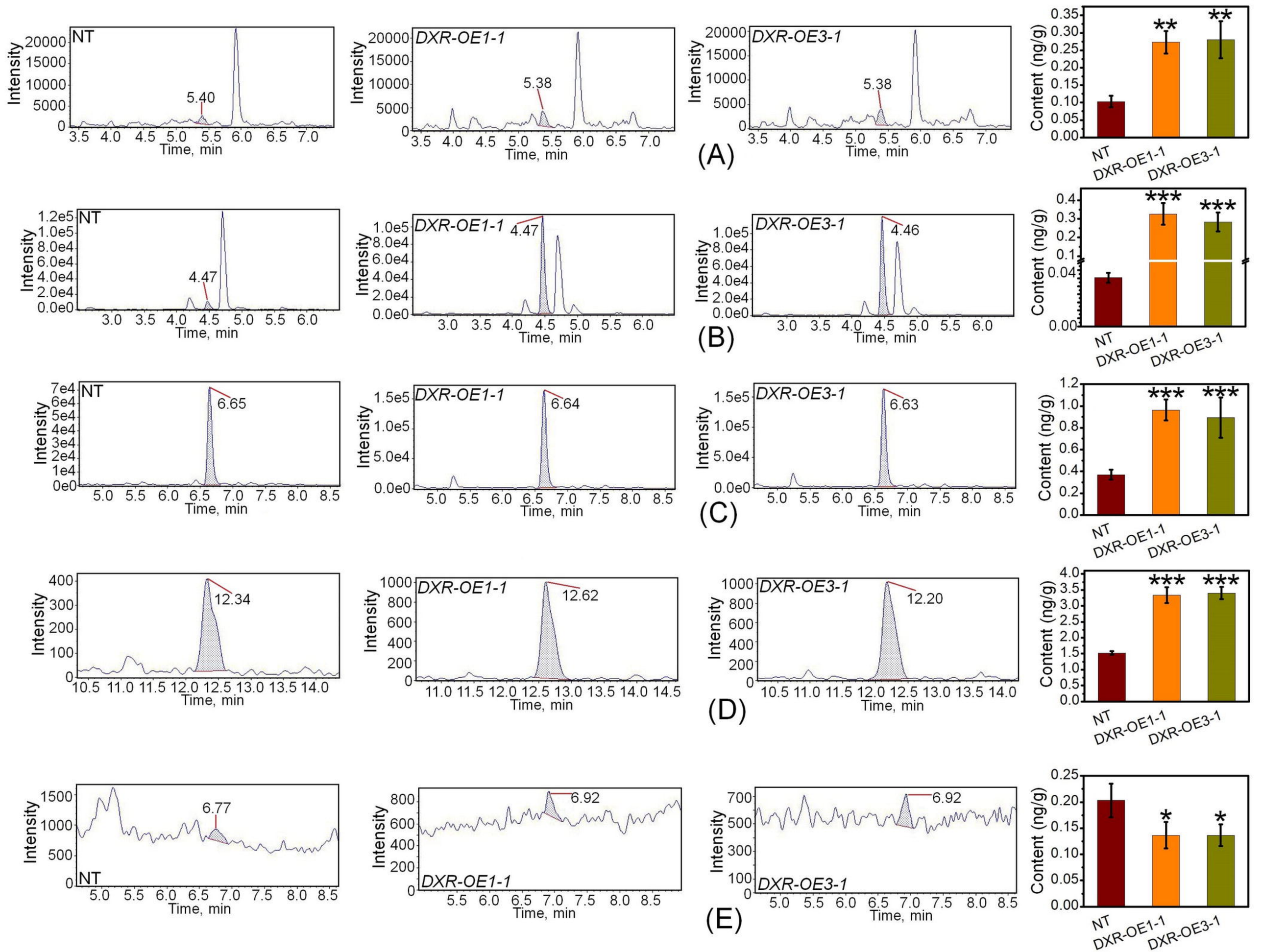
NT
DXR-OE1-1
DXR-OE3-1
5.40
5.38
5.38
Intensity
Time, min
Content (ng/g)
**
**
(A)
4.47
4.47
4.46
***
***
(B)
6.65
6.64
6.63
***
***
(C)
12.34
12.62
12.20
***
***
(D)
6.77
6.92
6.92
*
*
(E)